IEEE Access
Multidisciplinary | Rapid Review | Open Access Journal

Received March 16, 2020, accepted March 28, 2020, date of publication April 6, 2020, date of current version April 22, 2020.

Digital Object Identifier 10.1109/ACCESS.2020.2986048

Miniaturization of Dielectric Resonator Antenna by Using Artificial Magnetic Conductor Surface

SHAHID KHAN[1,2], HAZRAT ALI[3], MOHSEN KHALILY[2], (Senior Member, IEEE), SYED USMAN ALI SHAH[3], JALIL UR REHMAN KAZIM[4], HAIDER ALI[5], AND CAMEL TANOUGAST[1]

[1]Laboratoire-de-Conception-Optimisation-et-Modélisation-des-Systèmes (LCOMS), University de Lorraine, 57070 Metz, France
[2]Home of 5G Innovation Center (5GIC), Institute for Communication Systems (ICS), University of Surrey, Guildford GU2 7XH, U.K.
[3]Department of Electrical and Computer Engineering, COMSATS University Islamabad, Abbottabad Campus, Abbottabad 22060, Pakistan
[4]James Watt School of Engineering, University of Glasgow, Glasgow G12 8QQ, U.K.
[5]Department of Electronics Technology, University of Technology, Nowshera, Nowshera 24100, Pakistan

Corresponding author: Hazrat Ali (hazratali@cuiatd.edu.pk)

This work was supported in part by the 5G Innovation Center, University of Surrey, United Kingdom, and in part by the LCOMS Laboratory, University de Lorraine, France, under DrEAM mobility under Grant MDD/DrEAM/2019-06/N^{0}27.

ABSTRACT In this work, a dielectric resonator antenna (DRA) is miniaturized by using Artificial Magnetic conductor (AMC) surface without disturbing other important parameters. The design has three main features: (i) simple micro-strip line feeding, (ii) use of parasitic metallic strip to achieve impedance matching, and (iii) use of AMC surface for design miniaturization. The miniaturization is performed for dielectric resonator antenna at 3.5 GHz. Without changing the basic characteristic of the antenna such as gain, resonance frequency and efficiency, the size of the antenna was reduced by 85%. The AMC surface and DRA both are positioned on the FR4 substrate. The AMC surface consists of small patches of copper. DRA is mounted on the AMC surface, which significantly reduces the overall DRA volume. Nine AMC patches were introduced with a small gap between them. AMC patches were shorted with the ground metal with the help of small metallic vias. For an overall performance analysis, the design was fabricated, and measured results were taken. The fabricated design covers a bandwidth of 180 MHz for −10 dB reference value of the reflection coefficient, which is mainly used for 5G wireless application. The design has 14.2% impedance bandwidth. Based on the analysis made for the proposed design, it is found that this simple technique highly reduces the DR volume (85%) and ground surface (15.5%) while maintaining the overall performance of the square DRA.

INDEX TERMS Dielectric resonator antenna, artificial magnetic conductor, LTE, antenna miniaturization, metallic vias.

I. INTRODUCTION

For different wireless communication systems, the DRA volume is the major challenge. Provision of multiple and flexible features by communication systems must be accompanied by an adjustable DR front end. RF front end with an enlarged DRA volume makes it very difficult for the front end to be embedded into communication devices. Thus, the research community in the antenna design domain has always been motivated to develop newer designs and techniques for antenna miniaturization. In any communication system, front end occupies the key space and antenna is the integral part of the front end. After the introduction of semiconductor devices, there is an enormous decrease in the size of communication devices, but there is still a lot of work to be done on the reduction of the size occupied by RF front end and antenna.

The size reduction of antenna is not as simple as the design of the rest of the communication system because antenna design is governed by certain laws from Physics [1], [2]. Special techniques must be adopted to miniaturize the antenna size. Direct reduction in the antenna size without taking the support of some specific techniques can degrade the return loss, gain, and efficiencies and can shift the required resonance frequency. Thus, maintaining all the features and reducing the antenna size is very challenging.

The associate editor coordinating the review of this manuscript and approving it for publication was Muhammad Zulfiker Alam.

Different approaches and mechanisms can be incorporated to miniaturize the antennas. In [3], magnetic and dielectric components have been used to miniaturize antenna size. In [4] a mixture of magneto dielectric is utilized to reduce the antenna size. Using Electromagnetic Band gap can also be helpful in miniaturizing overall antenna size. The above-mentioned techniques are primarily used to miniaturize Microstrip Patch Antennas (MSA), which are of the same metallic nature.

During the last three decades, dielectric resonator antennas (DRAs) have highly attracted the attention of antenna designers. DRAs exhibit different features, which otherwise do not exist in MSA. The DRAs are three dimensional antennas with high radiation efficiency, compact size, low conductor losses, versatility in shapes and feeding mechanism [5]. These antennas are highly dependent on overall DR size and permittivity of the materials. A DRA made with low permittivity will have wide impedance bandwidth but will occupy large volume. Similarly, a DRA with higher relative permittivity will have smaller volume but will exhibit narrow impedance bandwidth [5].

For DRA miniaturization, very few techniques have been proposed in the literature. One mechanism is sticking high and low permittivity DRs together. In this technique, two DRAs with high and low values of permittivity correspondingly are sticked together to enhance the impedance bandwidth [6]. In [6], the size of the DR is not reduced but only bandwidth is enhanced, and the overall complexity of the design is increased. Another technique is sticking perfect electric conductor to the walls of the DR [7], [8]. In this case, some portion of the overall volume of the DR is reduced but at the same time radiation pattern is disturbed and gain is degraded because of the metallic nature of the PEC. Analyzing all the available techniques, it is concluded that we need to introduce some novel techniques which could reduce the complexity of the design, size of the DR and ground plane for the same impedance bandwidth and resonance frequency without degrading the overall performance.

Artificial magnetic conductor (AMC) surface has been in use for several applications. The unique characteristics of the AMC surface enhance the performance of the microwave devices. In most cases, AMC surface has been used for different applications jointly with microstrip patch antennas. Both these structures are metallic in nature and hence, can be integrated rather easily for a specific application. In [9], performance of the dual band planer microstrip antenna has been presented. The design is made up of the combinations of the common clothing and band gap substrates. The combination of these two structures reduced the absorption rate of the human body to 10 dB. A gain enhancement of 3 dBi was also observed. A good performance was witnessed when bent on human body. In [10], AMC surface has been used as an independent radiator for body area network. In [11], AMC surface has been used to improve the transmission enhancement between two antennas. Simulated and measured results show that by using AMC surface, mutual coupling has been largely improved between the two antennas. AMC surface can also be used to enhance the gain and bandwidth of the design. This application is specifically for micro strip patch antenna, which has low gain and narrow bandwidth. In [12], a lossy substrate is used which operates at 5GHz. This lossy substrate causes significant reduction in gain. By utilizing an array arrangement of 3×2, the gain of the system has been enhanced. RFID detection and improvement in the performance of the antenna can be achieved by using AMC surface array. Utilizing AMC surface beneath the RFID tag mainly enhances the performance of the RFIG tag in terms of reading distance of the tag, as reported in [13]. The wave reflected from the tag and AMC surface has constructive interference. Hence, the net received signal is stronger, which improves the distance for sensing the tag. AMC surface can widely be used for medical body area network. As discussed in [14], the AMC surface has been used with the antenna prototype on the arm of the user, which largely improves the reflection coefficient and impedance matching. AMC surface can be used for frequency re-configurability. This can be done by shifting the reflection phase of the AMC surface. Re-configurability through AMC surface is not the same as we do through active switches. In AMC surface, re-configurability is achieved by handling the AMC surface itself rather than handling the main radiator, which very often disturbs the radiation pattern, gain and efficiency in specific high impedance surface (HIS) active region. If we deploy active or passive switches, the re-configurability can be achieved in wide range of frequencies and also can be used for beam steering [15]–[17] and [10], [18], [19].

Dielectric resonators are semiconductor devices with different dielectric constant. Despite of having too many applications, there are only a few examples reported in the literature, which may prove the use of AMC surface with DR for different applications. Using AMC surface with a structure whose characteristics are very different is typically challenging and not explored before. The novelty of the design is to integrate both these independent resonant structures for the first time into a single resonance frequency structure for the size reduction of the overall design. To achieve this goal, a number of design and optimization techniques have been utilized.

In this work, AMC surface has been used to miniaturize the DRA at 3.5 GHz for 5G wireless application. This concept can be eventually extended to other wireless applications. The size of the DR and ground surface was miniaturized by 85% and 15.5% respectively while preserving the overall performances such as gain, efficiencies, bandwidth and resonance frequency. AMC structure consists of a number of small High Impedance Surface Unit Cell (HIS-UC) as presented in [20], [21]. After design of the single unit cell, the number is gradually increased to optimize its effect on the size of the DR and ground plane. The proposed design is significant in many ways. It has simple feeding technique with a better value of impedance matching, stable radiation pattern and more than 85% miniaturization is attained with a high value of gain. The

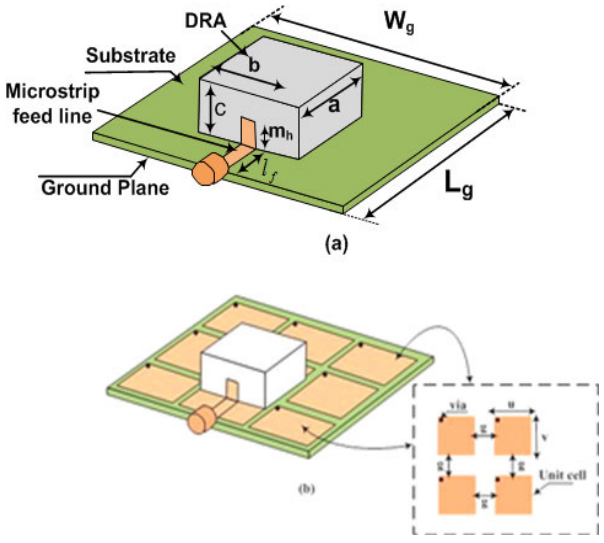

FIGURE 1. 3-D view of proposed antenna design: a) Without AMC and b) With AMC.

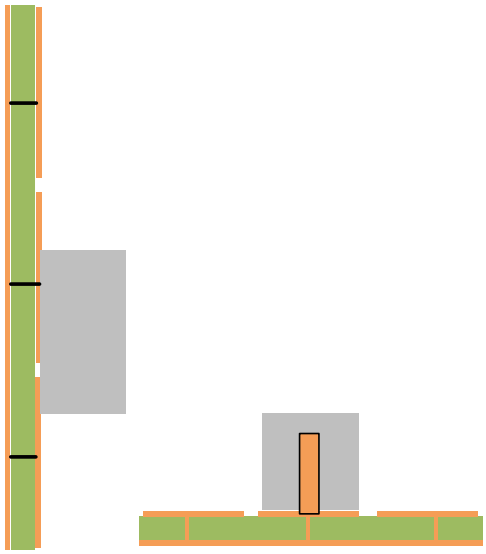

FIGURE 2. a) Side view b) Front view.

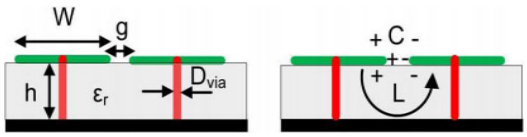

FIGURE 3. Artificial Magnetic Conductor design diagram.

rest of the paper is organized as follows: Section II presents the proposed design analysis, Section III presents parametric analysis, Section IV gives details of simulated and measured results and Section V concludes the paper.

A. PROPOSED DESIGN ANALYSIS

Initially a DR of dimensions a, b, c with relative permittivity, $\boldsymbol{\varepsilon_r} = 10$ is calculated for 3.5 GHz resonance frequency [5]. The different dimensions of DRA after using (1) were found to be a = 24mm, b = 22mm and c = 12mm.

The DR is positioned on FR4 substrate, which has a thickness of 1.6mm, relative permittivity (ε_r) = 4.4 and 0.002 tangent loss and an area of 60 × 60 mm^2. As given in Fig. 1, the DR is fed with a simple microstrip line of 3mm with 50Ω characteristic impedance. The feedline has a small gap of 0.1mm with AMC surface. A small metallic patch of 5.22 mm height is sticked to the wall of the DR, which improves the impedance matching and highly increases the value of reflection coefficient in terms of dB. Although there is no separate rigorous mathematical model available for DRA however we can take support of the following dielectric waveguide model (DWM) [5] to get the initial design of the un-miniaturized DRA.

$$TE^{y}_{1\delta 1} : f_r = \frac{C}{2\pi\sqrt{\epsilon_r}}\sqrt{K_x^2 + K_y^2 + K_z^2}$$
$$K_x = \frac{\pi}{a}; \quad K_z = \frac{\pi}{c}$$
$$K_y \tan\left(K_y\frac{b}{2}\right) = \sqrt{(\epsilon_r - 1)\left(K_0^2 - K_y^2\right)}, \qquad (1)$$

where, c is the speed of light, f_r is the resonance frequency and K_x, K_y, K_z are the wave numbers in the x, y, z directions. The three dimensions of the DR are a, b and c. The resonance frequency of the DRA calculated by using Equation 1for the given dimensions is 3.479 GHz which is then optimized to 3.5GHz (refer to [8]).

After calculating the DR dimensions, the next step is to optimize the AMC patch for the mentioned resonance frequency (3.5 GHz). To calculate the AMC patch area for the 3.5 GHz resonance frequency, Equation 2 is used.

$$f_r = \frac{1}{2\pi\sqrt{LC}} \qquad (2)$$

As shown in Fig. 3, L is the inductance and C is capacitance of AMC surface. L and C for the AMC patch are calculated by Equation 3 and Equation 4, as given in [22]:

$$C = \frac{W\varepsilon_0(1+\epsilon_r)}{\pi}\cosh^{-1}\left(\frac{w+g}{g}\right) \qquad (3)$$
$$L = 2\times 10^{-7}h\left[ln\left(\frac{2h}{r}\right) + 0.5\left(\frac{2r}{h}\right) - -0.75\right] \qquad (4)$$

where,

$$\mathrm{w} = 0.18\lambda_{3.5ghz}$$
$$\mathrm{g} = 0.01\lambda_{3.5ghz}$$
$$\mathrm{r} = 0.005\lambda_{3.5ghz}$$

As shown in Fig. 3, the thickness 'h' of the substrate is 1.6mm, the gap 'g' between two patches is 1.5mm, the radius 'r' of the via is 0.404mm. The calculated resonance frequency for AMC surface is 3.5 GHz. With the above calculation, the area of the patch V×U is found to be 15.17 × 15.17mm^2. Fig. 1(a) and Fig. 1(b) show the complete geometry of the

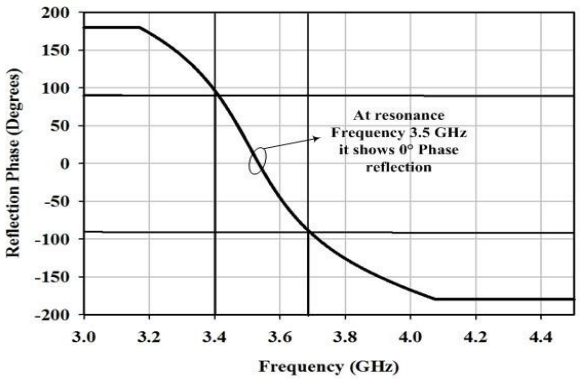

FIGURE 4. Phase reflection diagram.

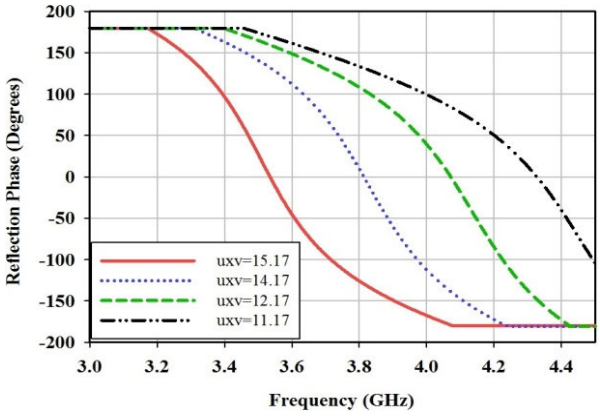

FIGURE 5. The effect of unit cell size on AMC unit cell reflection phase.

DRA without AMC and with AMC, whereas Fig. 2 (a) and Fig. 2 (b) describe the side and front view of the design.

After optimizing the AMC patch area, the number of patches were then increased to optimize the DRA miniaturization. It is observed that maximum miniaturization is attained at 3 × 3 arrangement of patches, which reduces the volume of DR by 85% and area of the ground surface by 15.5%.

Phase reflection of HIS Unit cell as shown in Fig. 4 is very important for the overall design [16]. It shows the idea of the Unit cell design for the specific resonance frequency. Zero crossings of the phase reflection show that unit cell is specifically working at the resonance frequency. From Fig. 4, it is also clear that zero crossing of the unit cell for this design is at 3.5 GHz.

II. PARAMETRIC STUDY

Parametric study generalizes the effect of different parameters on the simulated results. The parametric studies were conducted for the effect of unit cell area on the phase reflection, effect of DR location on the AMC surface, effect of strip height attached to the wall of the DR, effect of the gap between the two AMC unit cells and effect of the number of AMC unit cells on the overall simulated results.

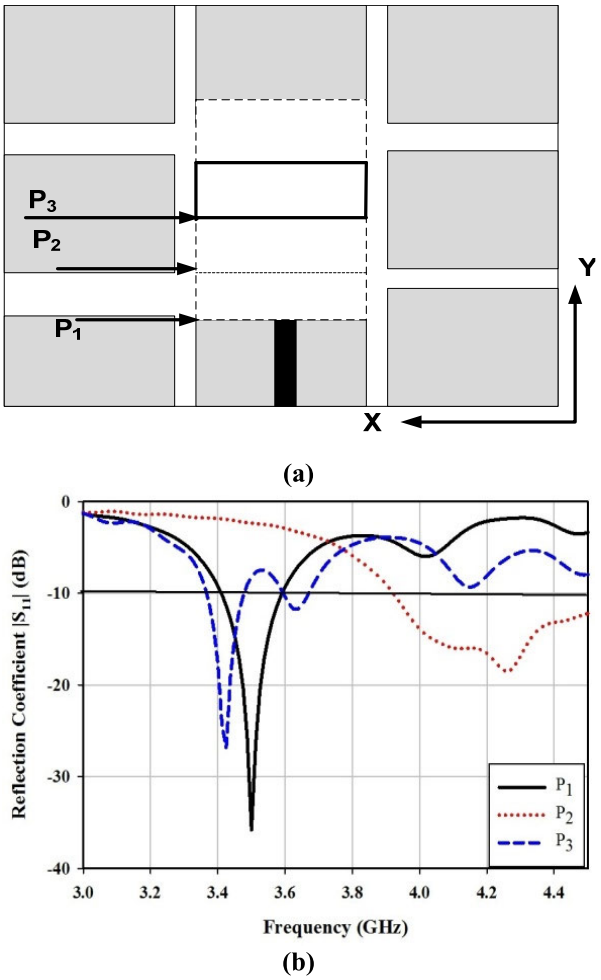

FIGURE 6. (a) Positions of DR on AMC surface and its effect on simulated results. (b) Positions of DR on AMC surface and its effect on simulated results.

A. EFFECT OF PATCH AREA

Fig. 5 shows the effect of patch area of the AMC unit cell on phase reflection. It is observed that when the patch area is increased, the resonance frequency for 0° reflection phase shifts to lower frequencies. Furthermore, the slope of the curve becomes steeper near the resonance frequency, which indicates a narrow bandwidth operations behavior of the AMC surface. Thus, a larger patch area leads to a larger capacitance C. This inversely affects the resonance frequency and shifts it to the lower frequencies.

B. EFFECT OF CHANGING THE POSITION OF DR ON REFLECTION COEFFICIENT

Fig. 6 a) shows the location of the DR at different positions. P1 (below center) antenna resonates at 3.5 GHz. By placing DR at position P2 (at center) the resonance at frequency shifts to 4.3 GHz. By placing the DR at position P3 (above center) the design resonates at 3.4 GHz. This shows that location of the DR along with other parameters also affect the resonance

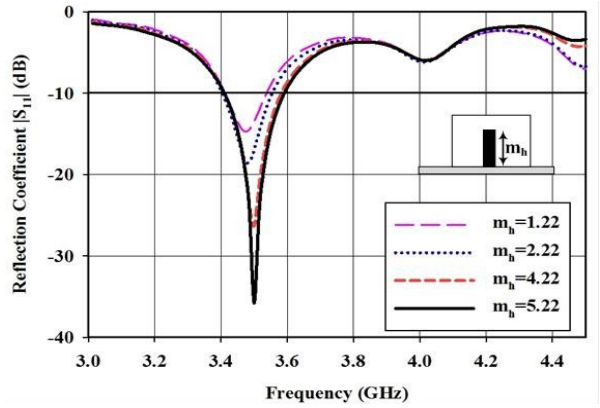

FIGURE 7. Simulated return loss (S_{11}) showing the effect of stacked strip.

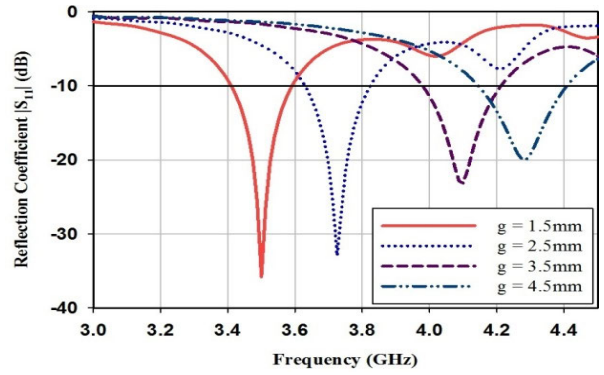

FIGURE 8. The effect of gap between unit cells on (S_{11}) reflection coefficient.

frequency. P1 is the final selected position, which gives us the required 3.5 GHz resonance frequency.

C. EFFECT OF CHANGING THE HEIGHT OF THE STICKED MICROSTRIP LINE

Fig. 7 shows the parametric analysis of varying the height of the microstrip feed line extended along the wall of DR for better impedance matching. The sticked microstrip is an extended feedline, which helps in coupling the energy into DR. This coupling of energy improves the impedance matching and maximizes the value of reflection coefficient. Simulated results show that by varying the length of the strip line, the impedance matching of the resonance frequency improves. Fig. 7 shows the reflection coefficient for different lengths of strip line. As the sticked patch height is increased the impedance matching is improved and maximum matching is achieved at 5.22mm. A better impedance matching is achieved at the strip length of 5.22mm with a reflection coefficient of −35 dB.

III. EFFECT OF GAP BETWEEN AMC UNIT CELS ON REFLECTION COEFFICIENT

Analysis of AMC surface is investigated by varying the gap between unit cells, which are connected to the ground through

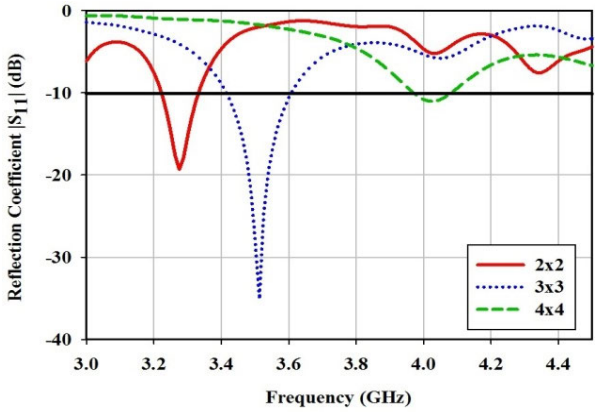

FIGURE 9. The effect of increasing or decreasing number of unit cells on resonance frequency.

small metallic vias. The results of the parametric analysis are depicted in the Fig. 8. While studying the effect of the gap between the patches, other parameters such as substrate permittivity, substrate thickness and vias radius and position remain unchanged. The gap between unit cells is varied from 1.5mm to 4.5mm.

Fig. 8 shows the simulated reflection coefficient (S11) of AMC surface with the different gap size. It is observed that when the gap is increased, the capacitance between metallic patches decreases and resonance frequency shifts towards the lower frequency and vice-versa. The analysis also shows that the patch area plays an important role in determining the resonance frequency.

A. EFFECT OF NUMBER OF AMC UNIT CELLS ON THE REFLECTION COEFFICIENT

Fig. 9 shows the simulated reflection coefficient (S11) of AMC surface with increasing or decreasing the number of array of unit cells. It is observed that when the number of unit cells on AMC surface is 2×2, the antenna resonates at 3.2 GHz with bandwidth of 120 MHz, which is not the desired frequency. By increasing the number of rows and columns to 3×3, the design resonates at 3.5 GHz with a bandwidth of 200 MHz. By further increasing the rows and columns to 4×4, the resonance frequency shifts to 4 GHz with an increase in the bandwidth. This shift of resonance frequency is observed because of changing values of the series equivalent capacitance. With the increase in the number of unit cells, there is a decrease in the series equivalent capacitance, which shifts the resonance frequency to higher range as given in Equation 2. In addition, the bandwidth is increased at higher frequencies because of the degrading quality factor as any change in the capacitances inversely affects the quality factor. Finally, a better impedance matching, desired bandwidth and miniaturization is achieved with 3×3 array of AMC surface.

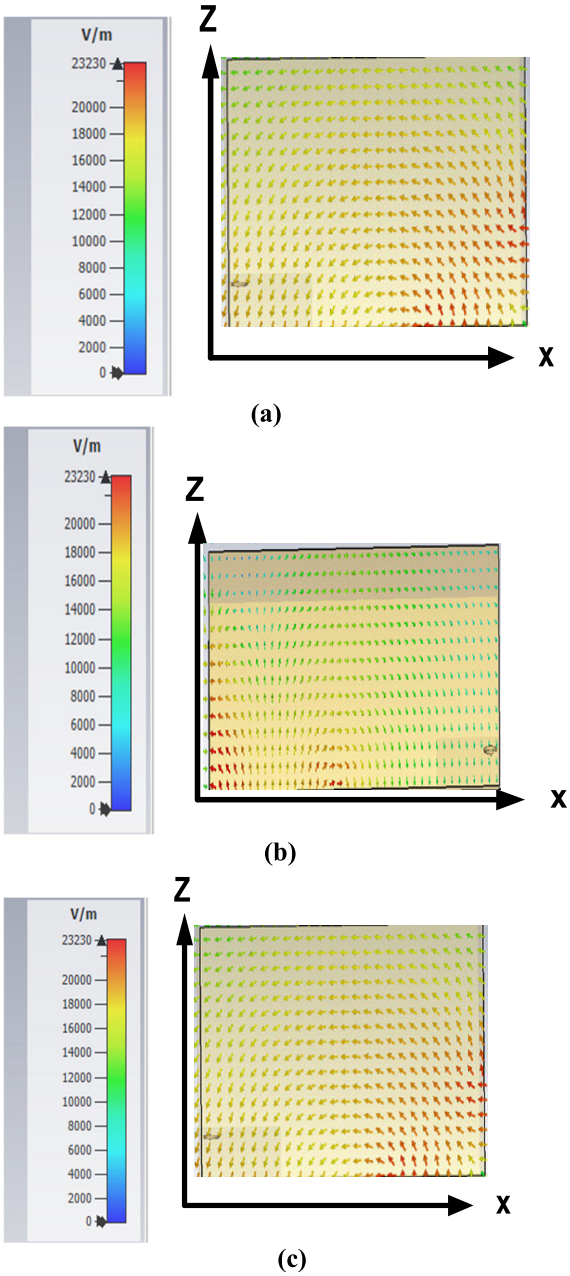

FIGURE 10. (a) X-Z plan E-field distribution inside DRA before miniaturization, (b) after miniaturization without AMC surface and (c) after miniaturization with AMC surface.

B. SIMULATED AND MEASURED RESULTS DISCUSSION

In this section, E-field distribution and operating modes inside the DR, reflection coefficient, gain and radiation pattern are discussed in detail.

For the simulated results validation, the design was fabricated. Fig. 10 provides presentation of the E-field distribution and operating modes inside the DR. Fig 10(a) shows that before miniaturization, the dominant mode inside the DR is $TE^{y}_{1\delta 1}$. Fig 10 (b) shows that direct miniaturization without the support of AMC surface changes the current distribution and the E-field inside the DR generates a higher order mode

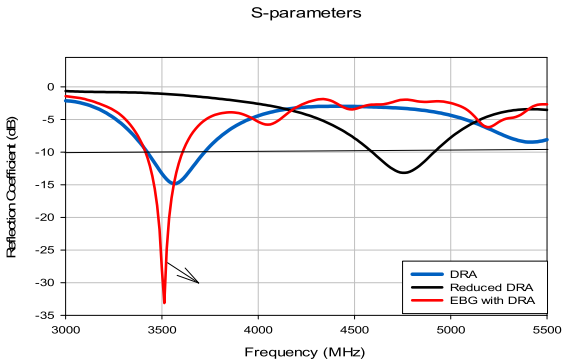

FIGURE 11. Simulated value of reflection coefficients.

(TE^{y}_{131}). Based on image theory, the operating mode inside DR is now (TE^{y}_{131}). Fig. 10(c) shows that when miniaturized DR is accompanied by the AMC surface, the initial field distribution and operating mode both are restored inside the DR which helps in achieving the initial resonance frequency. Fig. 11 shows the simulated reflection coefficients with and without AMC surface. Initially, the design with an un-miniaturized size operates at 3.5GHz. The antenna dimensions have an inverse relationship with the resonance frequency. Hence, when the antenna dimensions were reduced without being accompanied by the AMC surface, the resonance frequency jumped to the higher value with wide impedance bandwidth and low impedance matching. After adding AMC surface to the design, antenna restored its resonance frequency with much better impedance matching of -35dB. Also, a 30% reduction in the bandwidth and a slight shift in the resonance frequency is observed. This happens mainly due to the changing values of the capacitances with the addition of AMC surface. Besides, AMC is an independent resonant structure with a narrow bandwidth response. Generally, all metallic resonant structures have narrow bandwidth responses with good quality factor and impedance matching values. Reduction in the bandwidth will always be observed whenever we will use a DR of low permittivity, but radiation pattern will be stable with good value of impedance matching and gain. In case of DR of low permittivity, which has relatively narrow impedance, the bandwidth is hardly affected by AMC surface. In case of micro strip patch antennas, AMC surface enhances the overall bandwidth. Fig. 12 shows that without AMC surface, the prototype has a wider response at 3.5GHz. When AMC surface is introduced with the combination of the DR, the bandwidth is reduced. The measured reflection coefficient is slightly shifted towards higher frequencies because of fabrication inaccuracies. However, over all simulated and measured values are in close agreement. Table 2 summarizes the effect of AMC surface on the bandwidth of different structures.

Table 1 summarizes the overall performance of the design, including simulated and measured efficiencies, reflection coefficients and bandwidth. Even though there is slight difference between the simulated and measured gains, reflection

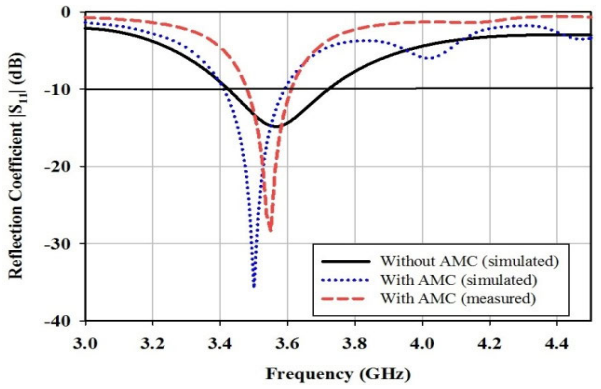

FIGURE 12. Simulated and measured Reflection coefficient without AMC at 3.576GHz and with AMC at 3.5GHz and 3.57GHz respectively.

TABLE 1. Performance summary of the design.

	Gain (dBi)		Efficiency (%)		Bandwidth (MHz)	
	Simulated	Measured	Simulated	Measured	Simulated	Measured
Without AMC	6.9	6.8	88	87	290	290
With AMC	6.87	6.64	74	71	200	180

coefficients and bandwidth with and without AMC surface nevertheless, the overall values are good enough for real time application. In Table 1, it is shown that there is a decrease in the efficiencies of the design. This decrease occurs because of the metallic nature of the AMC surface and the patch sticked to the wall of the DR. As both these two materials are conductors and their responses are highly frequency dependent. At high frequencies, more conductor losses are witnessed. Thus, a reduction in the overall efficiency of the design is observed. The final values of the efficiencies of the design after fabrication of the prototype are good enough for a real time use.

Table 1 also shows a reduction in the bandwidth of the design after the addition of the AMC surface. This reduction is because of the reduction in the equivalent series capacitance which increases the quality factor and reduces the bandwidth. Phase angle diagram of HIS surface also confirm the narrowing of the bandwidth with the addition of the AMC surface.

Fig. 13 shows the radiation pattern of the simulated and measured E-field and H-field. From the figure, it is clear that both E-field and H-field are broad side, and their radiation is focused towards 0°. The radiation pattern is stable with 6.87 dBi simulated and 6.64 dBi measured values of the gain. Table 1 also shows that there is slight difference between simulated and measured bandwidth. Simulated bandwidth is 200MHz while measured band is slightly narrow, which

TABLE 2. Performance summary of the design.

	DR of low permittivity + AMC surface	DR of high permittivity + AMC surface	Microstrip patch antenna + AMC surface
% Bandwidth	Decrement	Very little or no decrement	An Increment

TABLE 3. Dimension table before and after miniaturization.

Parameter	Without AMC (mm)3	With AMC (mm)3
Lg × Wg × *hc*	60 × 60 × 1.6	50 × 50 × 1.6
a × b × c	20 × 20 × 12	11 × 11 × 5

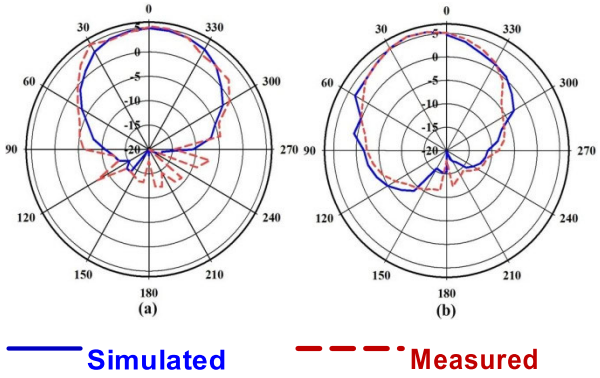

FIGURE 13. Simulated and measured radiation pattern (a) E-field on the left side and (b) H-field on the right side.

is 180 MHz. Fig. 14 shows the top and bottom view of the fabricated prototype. Fig. 15 shows the simulated and measured values of the gain in dBi at the operating frequency. For the whole operating bandwidth, the value of gain is stable. Moreover, simulated and measured values of the gain are in close agreement. Achieving this much high value of gain is an additional positive aspect of our proposed work.

Fig. 16 shows the simulated and measured values of the efficiencies. Measuring radiation efficiency is a post processing step after calculating Directivity and Gain in the anechoic chamber. Hence, the overall efficiency was measured relying on the software in the anechoic chamber. Radiation efficiency with simulated and measured values are good enough and stable. Due to metallic nature of the AMC surface, the value of efficiency is slightly less than the target value. In case of DR the minimum efficiency should be 0.90. In the proposed work, efficiency of the design is 0.87. Measured efficiency closely matches the simulated value. A minimum reduction is noticed which is due to the inaccuracies in fabrication and measurements.

Different techniques have been proposed to reduce the size of the Dielectric Resonator Antenna. Table 4 shows the

TABLE 4. Comparison of the proposed work with some published work.

Design reference	Antenna type	Permittivity	Antenna size	Height of the DR	Feeding mechanism	Design complexity	% Bandwidth	Maximum Gain of the design
[27]	Bridge shaped DRA	10	0.18λ×0.18λ×0.14 λ	0.14λ	Slot Coupled	Complex	16.8%	5.3dBi
[28]	Stacked DRA	10	0.017λ×0.017λ×0.012λ	0.012λ	Coaxial Probe	Complex	14.8%	2dBi
[29]	M-DRA	30, 10	0.16λ×0.17λ×0.10λ	0. 10λ	Coaxial Probe	Very Complex	2.7%, 30%	4.3dBi
[30]	R-DRA with tunnel	21	0.33λ×0.12λ×0.11 λ	0.11λ	Slot coupled	Complex	20.0%	7.2dBi
[31]	R-DRA	9.8	0.22λ×0.13λ×0.19λ	0.19λ	Micro strip feed line	Complex	23%	5.7dBi
[32]	F-DRA	10	0.36λ×0.56λ×0.07 λ	0.07λ	Micro strip feed line	Very complex	23%	5.0dBi
Proposed Design	AMC based R-DRA	10	0.12λ×0.12λ×0.058 λ	0.05λ	Micro strip feedline	Very simple	14.2%	6.87dBi

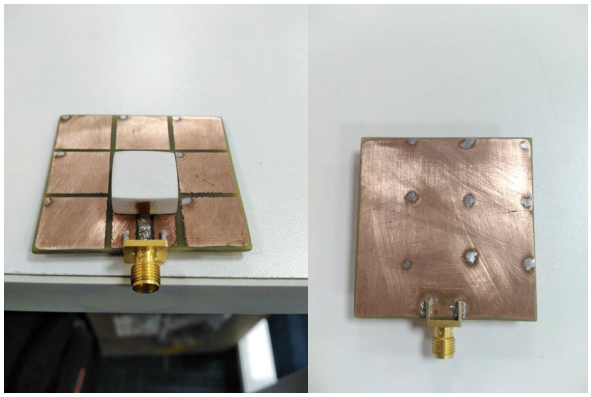

FIGURE 14. Fabricated design (a) top view (b) bottom view.

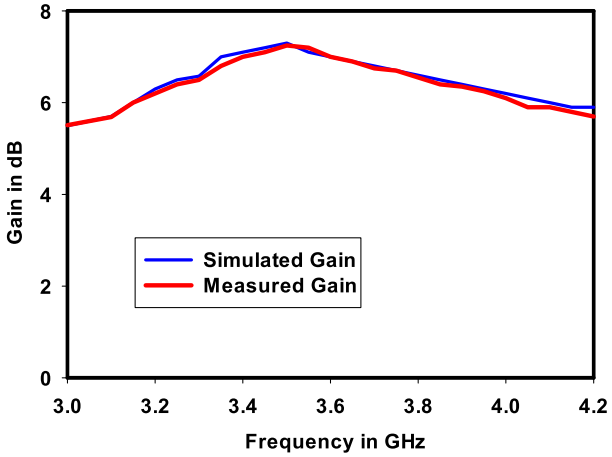

FIGURE 15. Simulated and measured gain of the prototype.

comparison of the similar work proposed in the literature for the size miniaturization of the Dielectric Resonator. In [27] a reduced size DRA composed of substrate of relative permittivity 10 is presented. The overall volume is $0.18\lambda \times 0.18\lambda \times 0.14\lambda$ and the height of the DR is 0.14λ. The overall design has complex nature with 16.3% bandwidth and 5.3 dBi gain. Similarly, in [28], a stacked DRA with $0.017\lambda \times 0.017\lambda \times 0.012\lambda$ volume is presented. The overall volume is bulky with low gain and complex design. In [29] a multiband DRA with $0.16\lambda \times 0.17\lambda \times 0.10\lambda$ and 0.10λ height is presented. The impedance bandwidths for both the designs are 2.7% and 30% respectively with 4.3dBi gain. The design is very bulky and complex. In [30] R-DRA with tunnel has been presented. The DRA is relatively smaller with 0.11λ height of the DR. But the design is still complex with a good value of gain. In [31] R-DRA with an overall volume of $0.22\lambda \times 0.13\lambda \times 0.19\lambda$ and height of 0.19λ is presented. The design is complex with 23% impedance bandwidth and 5dBi gain. In [32] a filtering DRA with wideband response is discussed. The overall volume is $0.36\lambda \times 0.56\lambda \times 0.07\lambda$ with 0.07λ height of the DR. The overall design is very complex with a good value of gain.

From Table 4, it is clear that the designs reported in [27]–[32] have achieved some miniaturization for DR but the final volume and height of the prototypes are still too large. The only exception is the design reported in [28], which has smaller electrical size as compared to the proposed work. The reason is using the DR of very high permittivity. If made with the DR of same permittivity the electrical size would have been far bigger than the proposed work. In the overall volume of the DR, one important aspect is the height of the DR as it then poses the issue of adjusting the prototype into the communication system. A second major issue that lowers the effectiveness of the above-mentioned works is the design

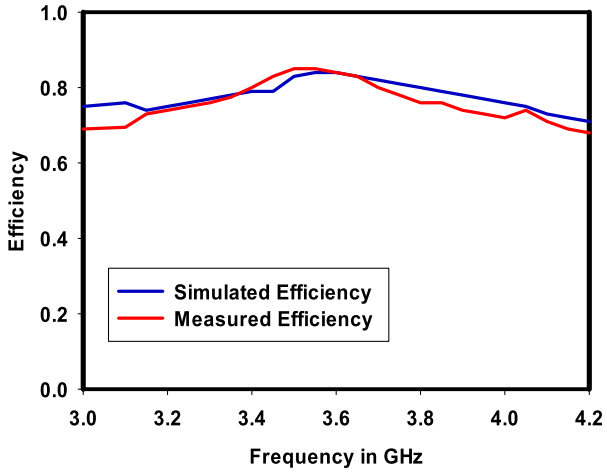

FIGURE 16. Simulated and measured efficiencies of the prototype.

complexity. A complex model is very difficult to fabricate, and inaccuracies in the design can lead to deviations from the simulated results. Moreover, the technique used for the DR miniaturization is reported by reducing the overall volume but the height of the DR, which is an important factor, remains the same. Also, the performance of the mentioned prototypes is hardly maintained. As a result, the final prototype has either disturbed radiation pattern or poor impedance matching with low values of the reflection co-efficient. In comparison to these designs, our proposed design offers several benefits. It has a very simple design structure with simple rectangular DR and micro strip patch feedline. To the best of our knowledge, the AMC surface has been used for the first time to reduce the volume of the DR and ground. The combination of AMC surface with DR has generated some very interesting results. The radiation pattern is much stable with a very good value of gain. The impedance bandwidth is slightly reduced because of the narrow bandwidth response of the AMC surface, but the value of the reflection coefficient is largely improved with very good matching values. Thus, the overall size of the DR is reduced by 85% with more than 50% reduction in the height of the DR. Moreover, the available bandwidth is good enough to support the targeted wireless applications.

IV. CONCLUSION

In this work, miniaturization of Dielectric Resonator Antenna with the help of AMC unit cell is presented. Previously, this technique was only applied to microstrip Patch Antennas. In this work, the proposed scheme is successfully applied to DR, which has different properties compared to microstrip patch antenna. The DRA is positioned on the 3×3 arrangement of the AMC unit cells. Simulated results are recorded for all the observations, which show that after applying AMC surface to the design, a significant reduction of 85% in the size of the DR is attained. The simulated design of the prototype is fabricated. Measured results are taken with the help of Vector Network Analyser (VNA) and anechoic chamber. Simulated and measured results reveal a good agreement, which shows the good performance and accuracy of the design.

REFERENCES

[1] H. A. Wheeler, "Fundamental limitations of small antennas," *IRE*, vol. 35, no. 12, pp. 1479–1484, Dec. 1947.
[2] W. Geyi, "Physical limitations of antenna," *IEEE Trans. Antennas Propag.*, vol. 51, no. 8, pp. 2116–2123, Aug. 2003.
[3] A. K. Skrivervik, J.-F. Zurcher, O. Staub, and J. R. Mosig, "PCS antenna design: The challenge of miniaturization," *IEEE Antennas Propag. Mag.*, vol. 43, no. 4, pp. 12–27, Aug. 2001.
[4] D. Kim, "Planar magneto-dielectric metasubstrate for miniaturization of a microstrip patch antenna," *Microw. Opt. Technol. Lett.*, vol. 54, no. 12, pp. 2871–2874, Dec. 2012.
[5] N. H. Shahadan, M. H. Jamaluddin, M. R. Kamarudin, Y. Yamada, M. Khalily, M. Jusoh, and S. H. Dahlan, "Steerable higher order mode dielectric resonator antenna with parasitic elements for 5G applications," *IEEE Access*, vol. 5, pp. 22234–22243, 2017.
[6] S. Danesh, S. K. A. Rahim, and M. Khalily, "A wideband trapezoidal dielectric resonator antenna with circular polarization," *Prog. Electromagn. Res. Lett.*, vol. 34, pp. 91–100, Oct. 2012.
[7] M. Khalily, M. K. A. Rahim, N. A. Murad, N. A. Samsuri, and A. A. Kishk, "Rectangular ring-shaped dielectric resonator antenna for dual and wideband frequency," *Microw. Opt. Technol. Lett.*, vol. 55, no. 5, pp. 1077–1081, May 2013.
[8] S. Khan, H. Ali, R. Khan, R. Harry, and C. Tanougast, "An L-shaped frequency reconfigurable MIMO dielectric resonator antenna for PCS band applications," in *Proc. 29th Irish Signals Syst. Conf. (ISSC)*, Belfast, U.K., Jun. 2018, pp. 21–22.
[9] S. Zhu and R. Langley, "Dual-band wearable textile antenna on an EBG substrate," *IEEE Trans. Antennas Propag.*, vol. 57, no. 4, pp. 926–935, Apr. 2009.
[10] Z. H. Jiang, D. E. Brocker, P. E. Sieber, and D. H. Werner, "A compact, low-profile metasurface-enabled antenna for wearable medical body-area network devices," *IEEE Trans. Antennas Propag.*, vol. 62, no. 8, pp. 4021–4030, Aug. 2014.
[11] K. Kamardin, M. K. A. Rahim, N. A. Samsuri, M. E. B. Jalil, and I. H. Idris, "Textile artificial magnetic conductor waveguide jacket for on-body transmission enhancement," *Prog. Electromagn. Res. B*, vol. 54, pp. 45–68, Nov. 2013.
[12] G. Shaker, H. Lee, K. Duncan, and M. Tentzeris, "Integrated antenna with inkjet-printed compact artificial magnetic surface for UHF applications," in *Proc. ICWITS*, 2010, pp. 1–4.
[13] I.-Y. Park and D. Kim, "Artificial magnetic conductor loaded long-range passive RFID tag antenna mountable on metallic objects," *Electron. Lett.*, vol. 50, no. 5, pp. 335–336, Feb. 2014.
[14] R. Otin and H. Gromat, "Specific absorption rate computations with a nodal-based finite element formulation," *Prog. Electromagn. Res.*, vol. 128, pp. 399–418, Jun. 2012.
[15] V. Sanchez and E. Paller, "A tunable artificial magnetic conductor using switched capacitance in a concentric overlapping geometry," in *Proc. IEEE Int. Antennas Propag. Symp. USNC/CNC/URSI North Amer. Radio Sci. Meeting*, Jun. 2003, pp. 439–442.
[16] F. Yang and Y. Rahmat-Samii, "Reflection phase characterizations of the EBG ground plane for low profile wire antenna applications," *IEEE Trans. Antennas Propag.*, vol. 51, no. 10, pp. 2691–2703, Oct. 2003.
[17] B. Liang, B. Sanz-Izquierdo, E. A. Parker, and J. C. Batchelor, "A frequency and polarization reconfigurable circularly polarized antenna using active EBG structure for satellite navigation," *IEEE Trans. Antennas Propag.*, vol. 63, no. 1, pp. 33–40, Jan. 2015.
[18] V. C. Sanchez and D. Wemiii, "Broadband antenna over electronically reconfigurable artificial magnetic conductor surfaces," U.S. Patent 6 917 343, Jul. 12, 2005.
[19] W. Yang, K.-W. Tam, W.-W. Choi, W. Che, and H. T. Hui, "Novel polarization rotation technique based on an artificial magnetic conductor and its application in a low-profile circular polarization antenna," *IEEE Trans. Antennas Propag.*, vol. 62, no. 12, pp. 6206–6216, Dec. 2014.
[20] D. Sievenpiper, L. Zhang, R. F. J. Broas, N. G. Alexopolous, and E. Yablonovitch, "High-impedance electromagnetic surfaces with a forbidden frequency band," *IEEE Trans. Microw. Theory Techn.*, vol. 47, no. 11, pp. 2059–2074, Nov. 1999.

[21] D. Sievenpiper, L. Zhang, R. F. J. Broas, N. G. Alexopolous, and E. Yablonovitch, "High-impedance electromagnetic surfaces with a forbidden frequency band," *IEEE Trans. Microw. Theory Techn.*, vol. 47, no. 11, pp. 2059–2074, Nov. 1999.
[22] R. Dewan, M. K. A. Rahim, M. R. Hamid, M. F. M. Yusoff, N. A. Samsuri, N. A. Murad, and K. Kamardin, "Artificial magnetic conductor for various antenna applications: An overview," *Int. J. RF Microw. Comput.-Aided Eng.*, vol. 27, no. 6, Aug. 2017, Art. no. e21105.
[23] D. Sievenpiper and J. Schaffner, "Beam steering microwave reflector based on electrically tunable impedance surface," *Electron. Lett.*, vol. 38, no. 21, pp. 1237–1238, 2002.
[24] D. F. Sievenpiper, J. H. Schaffner, H. J. Song, R. Y. Loo, and G. Tangonan, "Two-dimensional beam steering using an electrically tunable impedance surface," *IEEE Trans. Antennas Propag.*, vol. 51, no. 10, pp. 2713–2722, Oct. 2003.
[25] R. Dewan, M. K. A. Rahim, M. R. Hamid, H. A. Majid, M. F. M. Yusoff, and M. E. Jalil, "Reconfigurable antenna using capacitive loading to artificial magnetic conductor (AMC)," *Microw. Opt. Technol. Lett.*, vol. 58, no. 10, pp. 2422–2429, Oct. 2016.
[26] W. E. Mckinzie, III, "Reconfigurable artificial magnetic conductor using voltage controlled capacitors with coplanar resistive biasing network," U.S. Patent 6 525 695, Feb. 25, 2003.
[27] G. Almpanis, C. Fumeaux, and R. Vahldieck, "Dual-mode bridge-shaped dielectric resonator antennas," *IEEE Antennas Wireless Propag. Lett.*, vol. 9, pp. 103–106, Jan. 2010.
[28] R. Khan, J. U. R. Kazim, A. A. Khan, S. Aqeel, M. H. Jamaluddin, and O. U. Khalid, "Stacked-dielectric resonator antenna for TB white space application," *Micro Wave Opt. Lett. Technol. Lett.*, vol. 58, no. 9, pp. 2075–2079, 2016.
[29] R. Khan, J. U. R. Kazim, M. H. Jamaluddin, O. Owais, and J. Nasir, "Multiband-dielectric resonator antenna for LTE application," *IET Microw., Antennas Propag.*, vol. 10, no. 6, pp. 595–598, Apr. 2016.
[30] T.-H. Chang, Y.-C. Huang, W.-F. Su, and J.-F. Kiang, "Wideband dielectric resonator antenna with a tunnel," *IEEE Antennas Wireless Propag. Lett.*, vol. 7, pp. 275–278, 2008.
[31] A. Gupta and R. K. Gangwar, "Design, fabrication, and measurement of dual-segment rectangular dielectric resonator antenna array excited with conformal strip for S-band application," *Electromagnetics*, vol. 36, no. 4, pp. 236–248, May 2016.
[32] P. F. Hu, Y. M. Pan, X. Y. Zhang, and S. Y. Zheng, "A compact filtering dielectric resonator antenna with wide bandwidth and high gain," *IEEE Trans. Antennas Propag.*, vol. 64, no. 8, pp. 3645–3651, Aug. 2016.

SHAHID KHAN was born in Landikotal, Pakistan, in 1986. He received the B.S. degree in communication engineering from the University of Engineering and Technology Peshawar, Pakistan, and the M.S. degree in satellite navigation and related applications from Politecnico de Torino, Italy, in 2011. He is currently pursuing the Ph.D. degree with the University de Lorraine, France. Before joining the University de Lorraine, he worked as a Lecturer at COMSATS University Islamabad, Abbottabad, from 2012 to 2017. He is also a Visiting Fellow with the 5G Innovation Center, University of Surrey. He is working on the development of circularly polarized phased array DRAs for satellite application and reconfigurable dielectric resonator antenna for different wireless applications.

HAZRAT ALI received the B.Sc. and M.Sc. degrees in electrical engineering, in 2009 and 2012, respectively, and the Ph.D. degree from the University of Science and Technology Beijing, China, in 2015. He is currently an Assistant Professor with the Department of Electrical and Computer Engineering, COMSATS University Islamabad, Abbottabad Campus. At CUI, he is a member of the Signal Processing and Machine Learning Research Group. He is also the Head for digital signal processing course. His research interests lie in unsupervised learning, generative and discriminative approaches, and speech and medical image processing. He was a recipient of the HEC Scholarship, Top10 research pitch award, Kempe Foundation Sweden grant, the IEEE Student Travel Award, the IBRO grant, the TERENA/CISCO Travel grant, the QCRI/Boeing Travel grant, and the Erasmus Mundus STRoNGTiES research grant. He is selected as a Young Researcher at the 5th Heidelberg Laureate Forum, Heidelberg, Germany. He is an Associate Editor of the IEEE. He served as a Reviewer of IEEE Access, the IEEE Transactions on Neural Networks and Learning Systems, the IEEE Transactions on Medical Imaging, the IEEE Transactions on Emerging Topics in Computational Intelligence, *IET Signal Processing*, *Neural Processing Letters* (Springer), *ACM Transactions on Asian and Low Resource Language Information Processing, Computers and Electrical Engineering* (Elsevier), the *International Journal of Artificial Intelligence Tools, the Journal of Experimental and Theoretical Artificial Intelligence, Transactions on Internet and Information Systems*, and *Multimedia Tools and Applications* (Springer), and as a PC member at Frontiers of Information Technology conference (FIT 2016 and FIT 2019), ACL, MICCAI, INTAP 2019, INTELLECT 2019, ICACT 2019, ICACT 2018, ICACT 2017, and IEEE WiSPNet 2018.

MOHSEN KHALILY (Senior Member, IEEE) is a Lecturer in antenna and propagation with the Home of the 5G Innovation Centre (5GIC), Institute for Communication Systems (ICS), University of Surrey, U.K., where he was a Research Fellow on antennas and propagation, from December 2015 to March 2019. Prior to joining the 5GIC, he was a Senior Lecturer with the Wireless Communication Centre (WCC), University Technology Malaysia (UTM). He has published almost 100 academic articles in international peer-reviewed journals and conference proceedings. His research interests include large intelligent surface, 5G systems, dielectric resonator antennas, MIMO antennas, phased arrays, circularly polarized antennas for satellite application, hybrid beam-forming, leaky wave antennas, and mm-Wave&Terahertz antennas and propagation. He is a Fellow of the U.K. Higher Education Academy. He is also a member of the IEEE Antennas and Propagation Society, the IEEE Communication Society, and the IEEE Microwave Theory and Techniques Society, and an Associate Editor of IEEE Access.

SYED USMAN ALI SHAH received the bachelor's degree in telecommunication and networks from Hazara University, Pakistan, and the master's degree from COMSATS University Islamabad, Abbotabad Campus, in 2017. His has worked on a number of project including microstrip patch antennas, dielectric resonator antennas, and reconfigurable antennas.

JALIL UR REHMAN KAZIM was born in Nowshera, Pakistan, in April 1984. He received the bachelor's degree in electronics engineering from the University of Engineering and Technology Peshawar, Pakistan, in 2008, and the master's degree in electrical engineering from Linkoping University, Sweden, in 2012. He is currently pursuing the Ph.D. degree with the University of Glasgow, U.K. He authored or coauthored more than 20 article and conference papers. His research interest is in antenna design for different wireless applications.

HAIDER ALI was born in 1984. He received the B.S. degree in telecom engineering from NUCES, Pakistan, in 2007, and the M.S. and Ph.D. degrees in electronics engineering and the Ph.D. degree in electronics and communication engineering from Politecnico di Torino, Italy, in 2010 and 2014. He is currently working as an Assistant Professor with the Department of Electrical Engineering and Technology, University of Technology, Nowshera, Pakistan. His research interests include data acquisition systems, renewable energy materials, power electronics systems, design and development of antenna, radio frequency (RF) front end, and telecommunication subsystem for small satellites.

CAMEL TANOUGAST received the Ph.D. degree in microelectronic and electronic instrumentation from the Henri Poincaré University of Nancy, France, in 2001, and the authorization/accreditation to supervise research (HDR - Habilitation degree) from the University of Metz, in 2009. He is currently a Professor in electronics and embedded systems with the University of Lorraine, France. He joined the Electronic Architectures Group, Electronic Instrumentation Laboratory of Nancy, in 2003, and the Microelectronic and Sensor Interface Laboratory of Metz (LICM), in 2008. He has been the Head Research of the networked adaptive and self-organized systems at LICM. He joined the Laboratory of Design, Optimization and Modeling Systems (LCOMS), in 2013. He is currently the Deputy Director and the ASEC Team Leader of LCOMS for research in microelectronics, communicating embedded systems, and smart sensors. He has authored or coauthored more than 120 publications and several research books, participated to several editorial boards of books and international journals, and has been the Supervisor of 21 Ph.D. thesis. His research interests include radio communication, reconfigurable systems and NoCs, design and implementation real time processing architectures, optimization, and implementation design, System-on-Chip development, FPGA design, computing vision, image processing, cryptography, and the digital television broadcast (DVB).